Vapor Growth of Indium Monoiodide

Arne Cröll[a,b], Martin Volz[c], Vladimir Riabov[d] and Aleksandar Ostrogorsky[d]

[a] RSESC, University of Huntsville in Alabama, USA
[b] Kristallographie, University of Freiburg, Germany
[c] EM 31, NASA Marshall Space Flight Center, Huntsville, AL 35812, USA
[d] Armour College of Engineering, Illinois Institute of Technology, Chicago, USA

Introduction

Indium (I) iodide, InI, is part of a group of heavy metal iodides that can be used as room temperature radiation detectors [1-4]. Other examples are HgI_2, PbI_2, BiI_3, or $TlPbI_3$ [1]. InI has several advantages, such as low toxicity, no solid phase transition (such as in HgI_2), and no tendency to form polytypes (PbI_2, BiI_3). All binary iodides have layered structures and are quite soft, but InI is also the mechanically most stable compound of the binary compounds. Table 1 shows the main properties of InI in comparison with the other iodides and the most common room temperature radiation detector material, (Cd, Zn)Te.

InI is typically grown by the unseeded Bridgman method using a nucleation tip [5,6], but Czochralski (CZ) growth has also been demonstrated [7,8]. The resulting crystals have been used successfully for radiation detection, but both resistivity and mobility are usually well below theoretically predicted values.

Physical vapor transport (PVT), although much slower than melt growth, is an alternative method and has been used to grow e.g. HgI_2, PbI_2, BiI_3, CdTe. PVT growth should eliminate or reduce inclusions and impurities since it is based on sublimation, reduce intrinsic defects due to the lower growth temperature, and reduce dislocation densities due to reduced thermal and mechanical stress. As an example, PVT-grown CdTe showed a much improved structural quality compared to Bridgman- or THM-grown material [9, 10].

Table 1: Physical properties of metal iodides used for radiation detection in comparison to (Cd, Zn)Te

Material	(Cd,Zn)Te	BiI_3	InI	α-HgI_2	PbI_2	$TlPbI_3$
Average/High Z	49.1/52	60.5/83	51/53	62/80	62.7/82	64.4/82
N [cm^{-3}] Density [g cm^{-3}]	$1.48\cdot10^{22}$ 5.78	$5.90\cdot10^{21}$ 5.78	$1.32\cdot10^{22}$ 5.31	$8.48\cdot10^{21}$ 6.4	$8.05\cdot10^{21}$ 6.16	$5.02\cdot10^{21}$ 6.60
Band Gap [eV]	1.5-1.6	1.67	2.00	2.14	2.32	2.30
Resistivity [Ω cm]	10^{10}	10^{11}	10^{12}	10^{13} -10^{14}	10^{13}	10^{11}
Space Group/ Structure	$F\bar{4}3m - T_d^2$ Zincblende type	$R\bar{3} - C_{3i}^2$ Layered ⊥ **c**	$Cmcm - D_{2h}^{17}$ Layered ⊥ **b** TlI type	$P4_2/nmc - D_{4h}^{15}$ Layered ⊥ **c**	$P\bar{3}m1 - D_{3d}^3$ Layered ⊥ **c** CdI_2 type	$Cmcm - D_{2h}^{17}$ Perovskite related Not layered
Melting Point [°C]	1100	408	365	259 127 (ss phase tr.)	410	346
Bond Energy [eV]	1.10	2.26	3.43	0.36	2.04	
Hardness [MPa] Knoop/Vickers	HK 92	HV 12-15	HK 27	HK <10 HV 22	HgI_2<HK<10	HK 70
Crystal Growth Methods	Bridgman, THM, PVT	Bridgman, PVT	Bridgman, CZ, PVT	PVT, solution	Bridgman, CZ, PVT, solution, gel	Bridgman, PVT

Vapor Growth Setup

InI sublimates congruently, the vapor consists mostly of InI monomers [11,12]. Fig. 1 shows the calculated vapor pressures over solid and liquid InI as a function of temperature. The vertical growth ampoule is shown in fig. 2: A fused quartz frit holds the feed material above the cone-shaped fused quartz crucible, as shown in fig. 2. Both closed and semi-closed setups were used. Most ampoules were evacuated, a few employed 30mbar of Ar-based forming gas (4% H_2). A setup with the crystal on top, often employed in vapor phase growth, was not posssible due to the fact that the adhesion of the InI crystals to the ampoule wall is very weak.

The ampoules were placed in a 7-zone furnace originally built for Bridgman growth. Four thermocouples were placed on the outside of the ampoule at the positions of the nucleation tip, the rim of the growth cone, the frit, and the center of the feed material to control the temperatures during growth. Fig. 3 shows the ampoule positions with respect to the furnace temperature profile at the beginning and the end of growth, respectively.

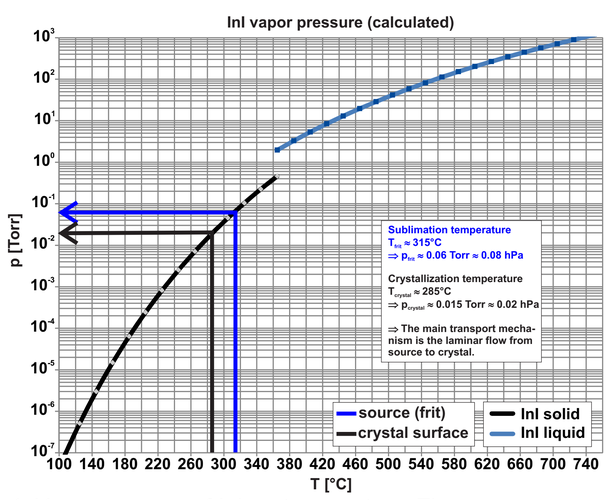

Fig. 1: Vapor pressure of InI vs. temperature. The melting point of InI is 365°C.

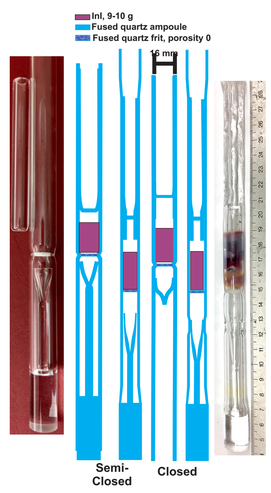

Fig. 2: Vapor growth ampoule designs.

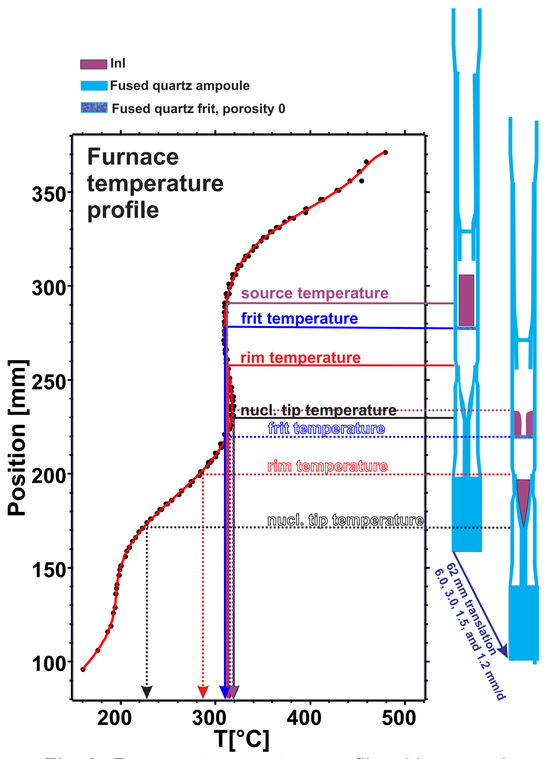

- *Fig. 3: Furnace temperature profile with ampoule positions at the beginning and the end of growth.*

The temperature profile of the six zone furnace has:

- Near isothermal conditions in the source region
- A temperature increase of 20-30K/cm above the source region to avoid or reduce sublimation into the empty space under the sealing plug
- A temperature "hump" of 5-7 K between source and the growth region, including nucleation tip and crucible rim
- A gradient zone to promote nucleation and growth in the translated ampoule with a gradient of approximately -20 K/cm.

The initial ampoule positioning in this profile results in a slightly inverted temperature profile at the beginning of the experiment (fig. 4) with the nucleation tip temperature ≥ rim temperature ≥ frit temperature. This allows the back sublimation of any possible nuclei in the tip/rim region left over from the ampoule filling and sealing process. Upward translation of the furnace then leads to a gradual transition to nucleation conditions in the crucible tip and subsequent growth.

The temperature "hump" between frit/source and crystal also facilitates

- a higher temperature at the rim of the crucible compared to the frit/source temperature during the initial and middle stages of growth to prevent nucleation there and
- stable growth and a convex interface [13,14]

Vapor Growth

After heating up the furnace and temperature stabilization at the TC positions, typically taking 6h, translation was initiated. To save time, the initial translation rate was 6mm/d, which was then reduced stepwise down to 1.5 or 1.2mm/d, as indicated by the grey curve in fig. 4.

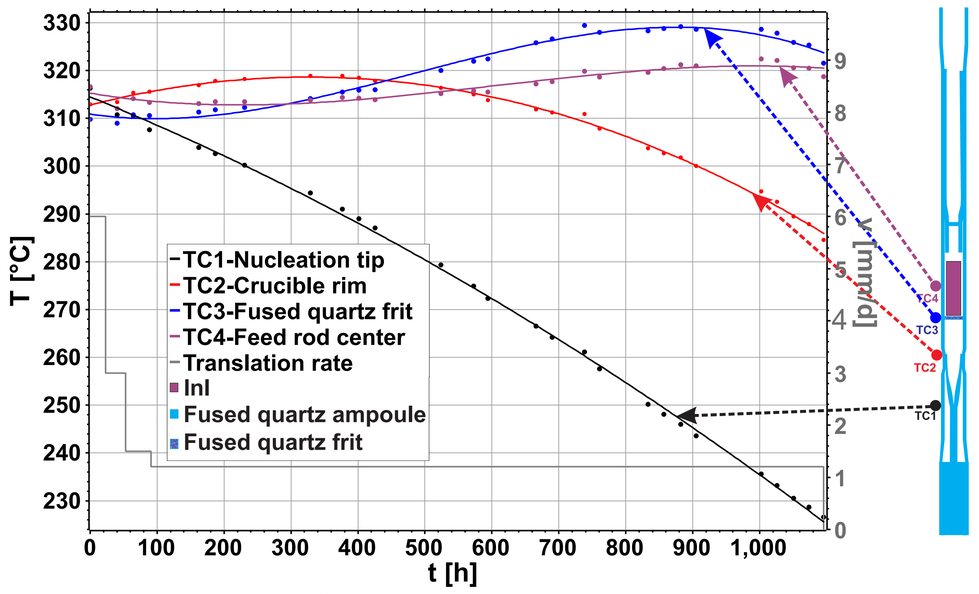

Fig. 4: Temperature evolution at the different TC positions during vapor growth, plus translation rates.

Vapor Growth Results

Typical growth times of 5-6 weeks resulted in crystals of 1.5-3cm length for both the closed and the semi-closed setup. The crystals are partially or completely faceted and transparent in the red region of the spectrum (figs. 5a,b). Structural and electric characterization of the crystals in comparison to Bridgman-grown crystals is planned.

Fig. 5a: InI crystals grown in a closed setup, vacuum, and at 1.2mm/d. The crystals are backlit to show the transparency.

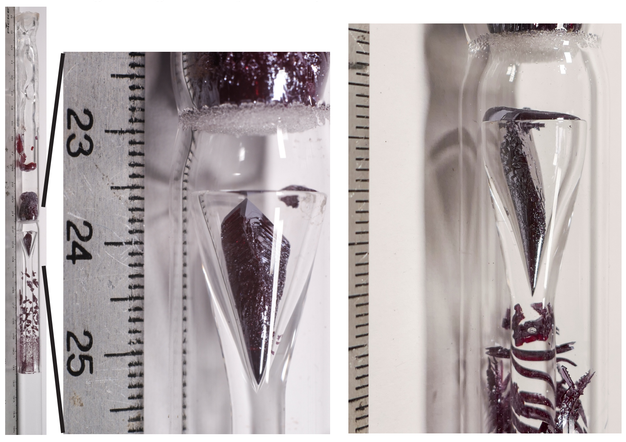

Fig. 5b: InI crystals grown in a semi-closed setup, 30 mbar forming gas, and at 1.5mm/d.

Thermal Properties of InI

In addition to the vapor growth, the anistropic thermal expansion of InI has been determined for temperatures between 25°C and 225°C by X-ray diffraction measurements of the 002, 200, and 080 diffraction peaks using a Panalytical X´Pert. diffractometer. Figs. 6 shows the change of the lattice constants with temperature. The RT values for the lattice constants were in very good agreement with the values from Meyer et al. [15] and also close to the values of Sidorov et al. [16], as indicated in the graphs. The resulting linear thermal expansion coefficents are: $\alpha_a=1.1\cdot10^{-5}$ K^{-1}, $\alpha_b=3.6\cdot10^{-5}$ K^{-1}, $\alpha_c=6.6\cdot10^{-5}$ K^{-1}. Sidorov et al. [16] determined the InI thermal expansion coefficients for the temperature range 51 K - 310 K. For RT, their values were: $\alpha_a=1.7\cdot10^{-5}$ K^{-1}, $\alpha_b=2.1\cdot10^{-5}$ K^{-1}, $\alpha_c=7.2\cdot10^{-5}$ K^{-1}, which is in reasonable agreement with our results. Several authors also proposed solid state phase changes for InI, at 150°C and 210°C [17-19], based on Raman spectroscopy [17] and DTA [18] measurements. Others authors [20, 21] disputed that, explaining the measured signals with InI_2 impurity reactions. Apart from the peak shift due to the lattice expansion, no change in the diffraction peak patterns with temperature was found in our measurements, i.e. no solid state phase change was detected.

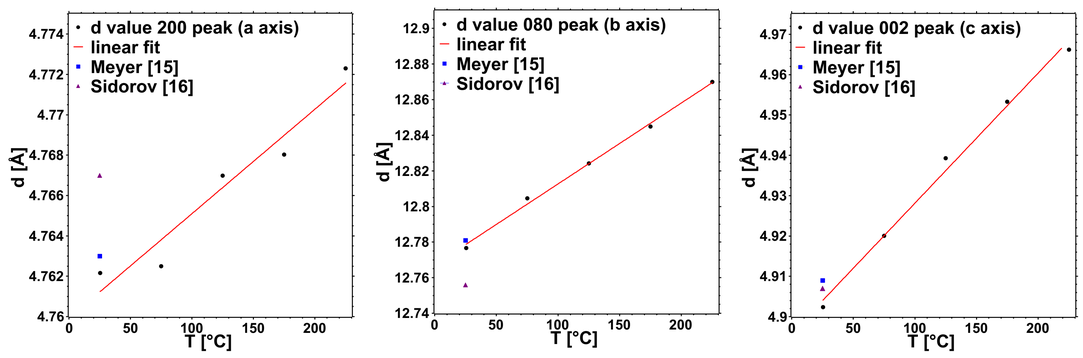

Fig. 6: Lattice constants of InI vs. temperature.

Acknowledgements

Financial support for this research by the ISS National Laboratory (formerly CASIS) and by the U.S. National Aeronautics and Space Administration Space Life and Physical Sciences Research and Applications Division under cooperative agreement NNM11AA01A is greatly appreciated. The authors would like to thank J. Quick for assistance with the translation setup.

References

[1] Owens, A.: Semiconductor radiation detectors. CRC Press, Boca Raton 2019
[2] Squillante, M.R., Zhou, C., Zhang, J., Moy, L.P., Shah, K.S.: InI nuclear radiation detectors. Proc. IEEE Conference on Nuclear Science Symposium and Medical Imaging, Orlando, FL 1992
[3] Shah, K.S, Bennett, P, Moy, L.P, Misra, M.M Moses, W.W: Characterization of indium iodide detectors for scintillation studies. Nucl. Instrum. Methods Phys. Res. A380 (1996), 215-219
[4] Onodera, T., Hitomi, K., Shoji, T.: Fabrication of Indium Iodide X- and Gamma-Ray Detectors. IEEE Trans. Nucl. Sci. 53 (2006), 3055-3059
[5] Bhattacharya, P., Groza, M., Cui, Y., Caudel, D., Wrenn, T., Nwankwo, A., Burger, A., Slack, G., Ostrogorsky, A.G.: Growth of InI single crystals for nuclear detection applications. J. Crystal Growth 312 (2010), 1228-1232
[6] Fedorov, P. P., Kuznetsov, S. V., Chuvilina, E. L., Gasanov, A. A., Plotnichenko, V. G., Popov, P. A., Matovnikov, A. V., Osiko, V. V.: Single-crystalline InI—Material for infrared optics. Dokl.Phys. 61 (2016), 261-265.
[7] Nicoara, I., Nicoara, D., Bertorello, C., Slack, G.A., Ostrogorsky, A. G., Groza, M., Burger, A.: Czochralski Growth of Indium Iodide and other Wide Bandgap Semiconductor Compounds. MRS Proc. 1341(2011).
[8] Xu, Zhaopeng, Zhang, Lei, Wang, Qian, Ji, Liangliang, Li, Ya-Ke: Horizontal Zone Refining of Indium Iodide (InI) Polycrystal. J. Inorg. Mater. 30 (2015), 1063-1068
[9] Laasch, M., Kunz, T., Eiche, C., Fiederle, M., Joerger, W., Kloess, G., Benz, K.W.: Growth of twin-free CdTe single crystals in a semi-closed vapour phase system. J. Crystal Growth 174 (1997), 696-707
[10] Kunz, T., Laasch, M., Meinhardt, J., Benz, K.W: Growth of twin-free CdTe single crystals in a semi-closed vapour phase system. J. Crystal Growth 184-185 (1998), 1005-1009
[11] Brumleve, T.R.; Mucklejohn, S.A.; O'Brien, N.W.: The preparation and vapour pressures of the indium(I) halides and the standard molar Gibbs free energy change for formation of InX from In(g) and X_2(g), (X = Cl, Br, or I). The Journal of Chemical Thermodynamics 21 (1989), 1193-1206
[12] Grinberg, Ya. Kh., Boryakova, V. A., Shevel'kov, V. F., Medvedeva, Z. S.: Evaporation and thermal stability of InI. Inorg. Mater. 8 (1972), 55-57
[13] Schönherr, E.: The investigation of the Pizzarello method with the theory of systems. J. Crystal Growth 92 (1988), 123-127
[14] Grasza, K., Janik, E., Mycielski, A., Bąk-Misiuk, J.: The optimal temperature profile in crystal growth from the vapour. J. Crystal Growth 146 (1995), 75-79
[15] Meyer, G. and Staffel, T.: Notiz zur Kenntnis der roten Monohalogenide des Indiums, InX (X = Cl, Br, I). Z. anorg. allg. Chem. 574 (1989), 114-118
[16] Sidorov, A. A., Kulchenkov, E. A., Popov, P. A., Prostakova, K. N., Fedorov, P. P., Kuznetsov, S. V., Chuvilina, E. L., Gasanov, A. A., Osiko, V. V.: Thermal expansion of InI crystal. Dokl.Phys. 61 (2016), 374-376.
[17] Ichikawa, K. and Fukushi, K.: Raman spectra of InI, InI_2 and InI_3. Correlation between structure and thermodynamic properties of fused InI_3 - InI_2 mixtures. J. Chem. Soc., Faraday Trans. 1 76 (1980), 291-301
[18] Gulieva, T. N.: Synthesis and Investigation of indium iodide. Izvestiia vysshikh uchebnykh zavedenii. Khimiia i khimicheskaia tekhnologiia 34 (1991), 7-10
[19] Hansen, S. C. and Kobertz, D.: Solid-State Transformations in Metal Iodides. Solid State Phenomena 38 (2008), 29-42
[20] Смирнов, В. А. Дмитриев, В. С., Редькин, А. Н.: Химия одновалентного индия. Наука /Nauka, Moscow 1986
[21] Fedorov, P. P., Popov, A. I., Simoneaux, R. L.: Indium iodides. Russ. Chem. Rev. 86 (2017), 240-286